STIMULUS REPORT

blood advances

Defenestrated endothelium delays liver-directed gene transfer in hemophilia A mice

Tomasz W. Kaminski,[1] Eun-Mi Ju,[1] Shweta Gudapati,[1] Ravi Vats,[1,2] Sanya Arshad,[1] Rikesh K. Dubey,[1] Omika Katoch,[1] Egemen Tutuncuoglu,[1] Jonathan Frank,[3] Tomasz Brzoska,[1,4] Donna B. Stolz,[4] Simon C. Watkins,[3] Stephen Y. Chan,[1,5] Margaret V. Ragni,[1,4,6] Enrico M. Novelli,[1,4] Prithu Sundd,[1,2,5] and Tirthadipa Pradhan-Sundd[1,2,4]

[1]Pittsburgh Heart, Lung and Blood Vascular Medicine Institute, University of Pittsburgh School of Medicine, Pittsburgh, PA; [2]Department of Bioengineering, and [3]Department of Cell Biology, University of Pittsburgh, Pittsburgh, PA; [4]Division of Hematology/Oncology, and [5]Division of Pulmonary Allergy and Critical Care Medicine, Department of Medicine, University of Pittsburgh School of Medicine, Pittsburgh, PA; and [6]Hemophilia Center of Western Pennsylvania, Pittsburgh, PA

Key Points

- FVIII knockout mice manifest delayed AAV8-mediated gene transduction in the liver.
- The delayed liver-directed gene transduction in FVIII knockout mice is associated with loss of sinusoidal endothelial fenestration.

Hemophilia A is an inherited bleeding disorder caused by defective or deficient coagulation factor VIII (FVIII) activity. Until recently, the only treatment for prevention of bleeding involved IV administration of FVIII. Gene therapy with adeno-associated vectors (AAVs) has shown some efficacy in patients with hemophilia A. However, limitations persist due to AAV-induced cellular stress, immunogenicity, and reduced durability of gene expression. Herein, we examined the efficacy of liver-directed gene transfer in FVIII knock-out mice by AAV8-GFP. Surprisingly, compared with control mice, FVIII knockout ($F8^{TKO}$) mice showed significant delay in AAV8-GFP transfer in the liver. We found that the delay in liver-directed gene transfer in $F8^{TKO}$ mice was associated with absence of liver sinusoidal endothelial cell (LSEC) fenestration, which led to aberrant expression of several sinusoidal endothelial proteins, causing increased capillarization and decreased permeability of LSECs. This is the first study to link impaired liver-directed gene transfer to liver-endothelium maladaptive structural changes associated with FVIII deficiency in mice.

Introduction

Hemophilia A is an X-linked recessive bleeding disorder caused by defective or deficient coagulation factor VIII (FVIII).[1,2] Affected individuals are at risk for spontaneous bleeding into joints, which can lead to persistent arthropathy.[1,3] Current therapy primarily relies on the administration of exogenous FVIII, which is inconvenient, does not fully prevent breakthrough bleeding, and fosters the development of inhibitor alloantibodies.[1] Recent advancements in liver-directed gene transfer suggest that gene therapy can be a potential cure for hemophilia A.[4,5] Adeno-associated virus (AAV) -based liver-directed gene therapy is the current approach in hemophilia A,[6] and various clinical trials to assess the efficacy and safety of gene therapy in patients are now in progress.[4,7,8] The enormous size of the FVIII coding sequence and the suboptimal synthesis of FVIII protein post–gene therapy are 2 persistent challenges of gene therapy approaches.[5,9] Moreover, immunogenicity of recombinant FVIII[10] and FVIII overexpression eliciting a cellular stress response are other major concerns.[11] The FVIII total knockout ($F8^{TKO}$) mouse is an ideal model for evaluating novel hemophilia A gene therapies.[12] AAV-mediated FVIII gene transduction is effective, although with a transient response in $F8^{TKO}$ mice.[13] In this study, we evaluated the stability and efficacy of a liver-driven gene transfer approach in $F8^{TKO}$ mice[14] using a recombinant AAV8 vector. We used

Submitted 18 October 2021; accepted 31 March 2022; prepublished online on *Blood Advances* First Edition 15 April 2022; final version published online 23 June 2022. DOI 10.1182/bloodadvances.2021006388.

Requests for data sharing may be submitted to Tirthadipa Pradhan-Sundd (tip9@pitt.edu.).

The full-text version of this article contains a data supplement.

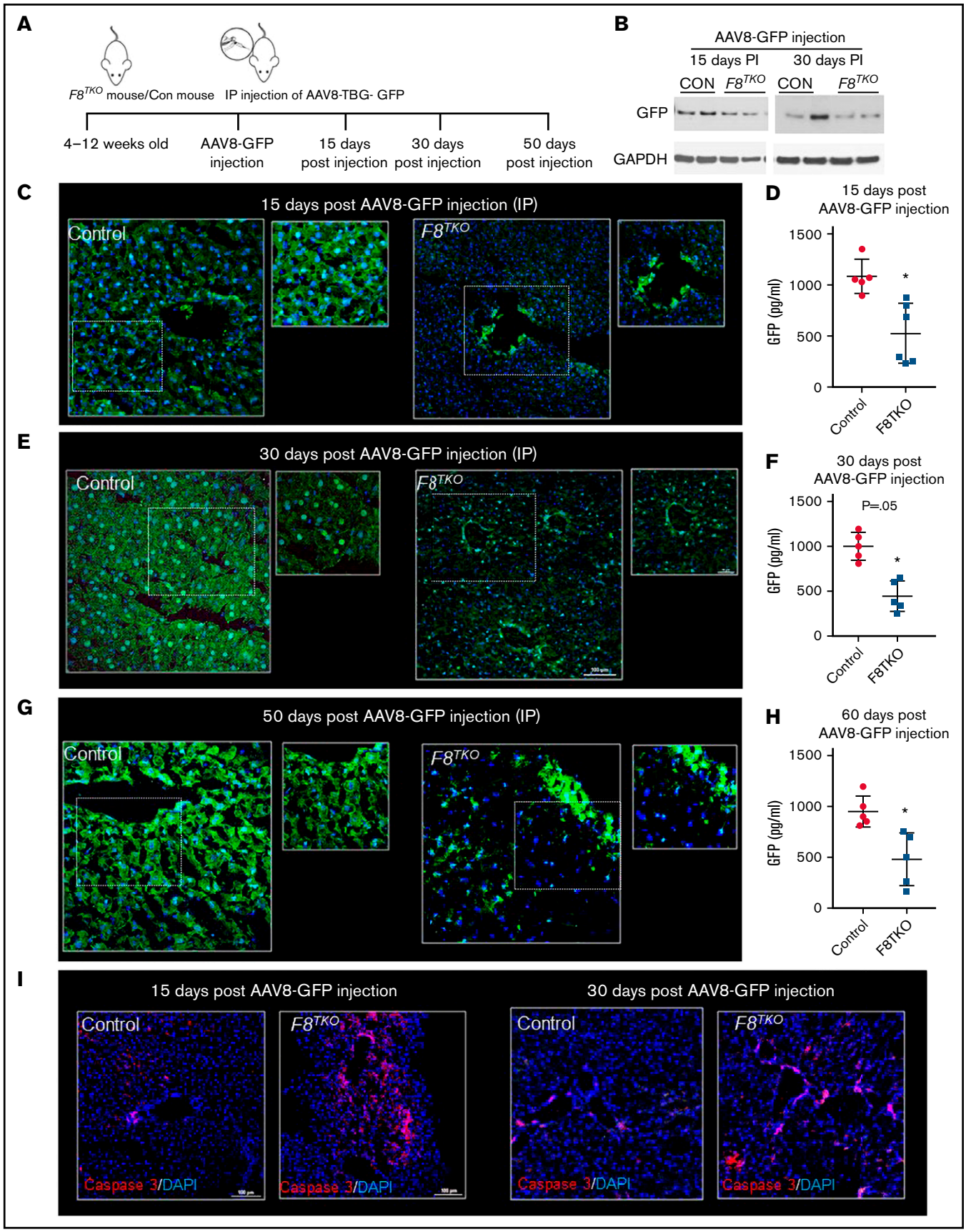

Figure 1.

green fluorescent protein (GFP) as a model gene for transduction because of its small size and lack of known adverse effects in the liver. Interestingly, when compared with littermate control mice, liver-directed gene transfer was significantly delayed in $F8^{TKO}$ animals. Remarkably, the delay in liver-directed gene transfer in $F8^{TKO}$ mice was associated with an absence of liver sinusoidal endothelial cell (LSEC) fenestration, which can lead to altered expression of major endothelial proteins, causing increased capillarization and decreased permeability of LSECs.

Methods

Animals

FVIII total knockout mice ($F8^{TKO}$) on C57BL/6J background were a generous gift from Pete Lollar. For these studies, we used $F8^{TKO}$ male mice[14] and age-matched unaffected littermate controls, heterozygous females generated by crossing homozygous $F8^{TKO}$ mice with C57BL/6J mice. AAV8–thyroid-binding globulin (TBG)-GFP was obtained from Vector Biolabs. Four-week-old $F8^{TKO}$ male mice were given an intraperitoneal (IP) injection of 1×10^{12} genome copies of AAV8–TBG-GFP. Twelve-week-old $F8^{TKO}$ null mice were given a single intravascular injection of 5×10^{11} genome copies of AAV8–TBG-GFP per mouse. A second line of FVIII-KO, B6; 129S-F8tm1Kaz/J strain and littermate controls were obtained from Jackson Laboratory. Twelve-week-old B6; 129S-F8tm1Kaz/J mice and controls were given a single intravascular injection of 5×10^{11} genome copies of AAV8–TBG-GFP. All animal experiments were approved by the Institutional Animal Care Committee at the University of Pittsburgh.

SEM and transmission electron microscopy

For scanning electron micrography (SEM), whole liver was perfused and fixed in glutaraldehyde. The surgical and perfusion techniques have been described previously.[15] Slides were examined with a JEM-1011 transmission electron microscope at 80 kV.

Liver intravital imaging

The surgical procedure has already been published in detail.[15] Texas red (TXR)-dextran (200 g) or AF488-anti-CD31 (100 g) was used as intravascular fluorescent dyes. A Nikon MPE-multiphoton excitation microscope was used for microscopy at the Center for Biological Imaging at the University of Pittsburgh.

Statistical analysis

All comparisons between the 2 groups were deemed statistically significant by an unpaired, 2-tailed Student t test (*$P < .05$; **$P < .01$). Additional methods used in this study are standard and are described in the supplemental data.

Results and discussion

To examine the efficacy, stability, and safety of AAV-mediated liver-directed gene transfer in $F8^{TKO}$ mice, AAV8–TBG-GFP was administered IP, and GFP expression was analyzed in the liver 15 and 30 days postinjection (Figure 1A-B). Previously, we showed that AAV8–TBG-GFP (at a dose of 1×10^{12} genome copies) can successfully transfer to the liver within 10 to 12 days.[16] Surprisingly, immunofluorescence (Figure 1C) of GFP at day 15 postinjection revealed significantly fewer GFP^+ cells in the liver of $F8^{TKO}$ compared with control mice. Only large hepatic veins contained GFP^+ cells in the $F8^{TKO}$ liver (Figure 1C). Whole-liver enzyme-linked immunosorbent assay (ELISA) also indicated that GFP expression in the liver was significantly lower in $F8^{TKO}$ compared with control mice (Figure 1D). Similar to the 15-day timepoint, we identified fewer GFP^+ cells in $F8^{TKO}$ liver 30 days postinjection (Figure 1E). On day 30, however, the total percentage of GFP^+ cells was higher than on day 15 (Figure 1E-F; supplemental Figure 1A), but it remained significantly lower when compared with control mice. Notably, we still found GFP staining in the large hepatic veins in $F8^{TKO}$ mice that was not present in control liver at day 30 postinjection (Figure 1E). Finally, the reduced GFP expression was confirmed using a Western blot assay, which revealed consistently low GFP protein expression in $F8^{TKO}$ liver compared with controls on days 15 and 30 postinjection (Figure 1B). Consistent with IP injection, IV injection, even at a lower dose, resulted in a similar delay in GFP transduction in $F8^{TKO}$ animals at 8 weeks as seen by both immunofluorescence (Figure 1G), ELISA (Figure 1H), and western blot assays (supplemental Figure 1F). Identical to $F8^{TKO}$ mice, a second strain of FVIII-deficient mice (*B6; 129S-F8tm1Kaz/J*) exhibited a similar delay in AAV8-GFP transduction compared with control mice at 8 weeks following IV administration of AAV8-GFP (supplemental Figure 1C-E).

The recombinant AAV8-vector efficiently transduces target tissues by passing across[17] the permeable barrier of endothelial cells.[18] We hypothesized that the reduced GFP transduction in $F8^{TKO}$ mice was due to endothelial cell death upon AAV8 administration. Supporting our hypothesis, caspase-3 staining revealed significant enrichment in the liver of $F8^{TKO}$ mice compared with control mice after AAV8-GFP administration at both the 15- and 30-day timepoints (Figure 1I). To further confirm apoptosis of LSECs, we next used liver intravital imaging to visualize LSECs in $F8^{TKO}$ mice at baseline and upon AAV8-GFP administration. TXR-dextran (red) and AF488–anti-CD31 antibody (green) were IV administered to visualize

Figure 1 (continued) AAV8-driven liver-directed gene transfer is significantly delayed in hemophilia A mice. (A) Schematic showing delivery of AAV8–TBG-GFP to hemophilia A ($F8^{TKO}$) or control (unaffected littermate heterozygous) mouse. (B) Western blot analysis of GFP in control and $F8^{TKO}$ mice after 15- and 30-days post–AAV8-GFP administration (IP). (C) Immunofluorescence of GFP staining in control and $F8^{TKO}$ mice 15 days post–AAV8-GFP injection (IP). The dotted regions are zoomed in as inset. (D) ELISA assay of total liver GFP amount in control and $F8^{TKO}$ at 15 days post–AAV8-GFP injection ($P = .04$). (E) Immunofluorescence of GFP staining in control and $F8^{TKO}$ mice 30 days post–AAV8-GFP injection (IP). The dotted regions are zoomed in as inset. (F) ELISA assay of total liver GFP amount in control and $F8^{TKO}$ 30 days post–AAV8-GFP injection ($P = .06$). (G) Immunofluorescence of GFP staining in control and $F8^{TKO}$ mice 60 days post–AAV8-GFP injection (IV). The dotted regions are zoomed in as inset. (H) ELISA assay of total liver GFP amount in control and $F8^{TKO}$ at 60 days post–AAV8-GFP injection ($P = .07$). (I) Immunofluorescence for caspase-3 showed an increased accumulation in $F8^{TKO}$ mouse liver 15- and 30-days post–AAV8-GFP administration, which was not seen in matched control liver. All control mice used were unaffected littermate heterozygoes mice.

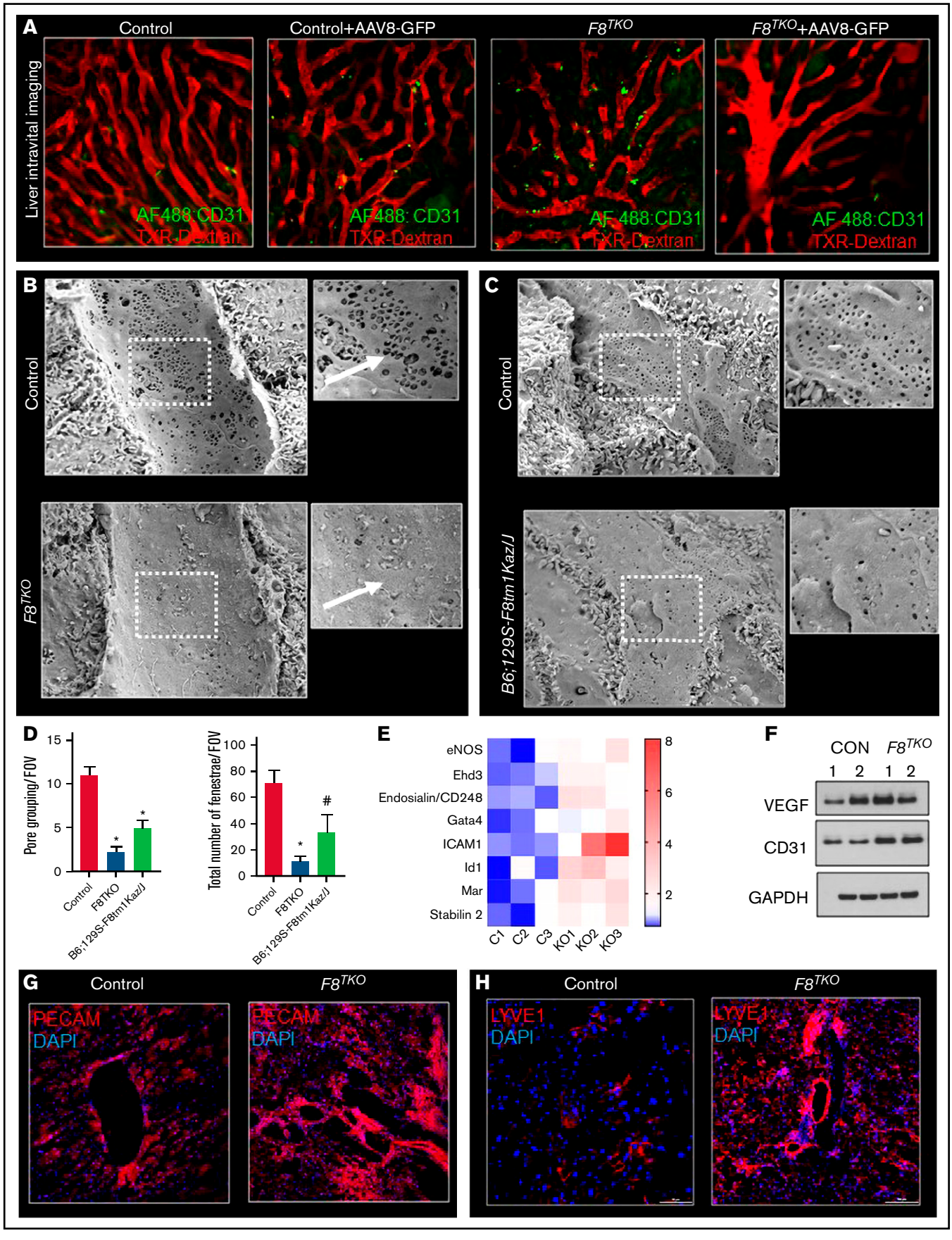

Figure 2.

hepatic blood flow and LSECs, respectively. At baseline, both control and $F8^{TKO}$ mice showed normal blood flow and enriched expression of AF488–anti-CD31 (Figure 2A). However, there were fewer AF488–anti-CD31^{+}endothelial cells in $F8^{TKO}$ than control mice at day 15 post–AAV8-GFP treatment (Figure 2A), suggestive of apoptosis of LSECs in $F8^{TKO}$ mice post–AAV8-GFP administration.

We hypothesized that the reduced GFP transduction and increased apoptosis of LSECs in $F8^{TKO}$ mice were caused by endogenous endothelial structural changes that prevented molecule passage to the liver.[19] To gain access to the liver parenchyma, liver-directed molecules typically pass through fenestrae present in LSECs.[17,20] As the diameter of LSEC fenestrations is smaller than the resolution of standard light microscopy, we used SEM to visualize them. As shown in Figure 2B-D, the endothelial fenestration in the liver of $F8^{TKO}$ and *B6; 129S-F8tm1Kaz/J* mice was dramatically reduced compared with control mouse liver. Furthermore, grouping of fenestrae and overall pore size were also reduced in $F8^{TKO}$ mice as well as *B6; 129S-F8tm1Kaz/J* mice (Figure 2B,D). The absence of fenestrae has been associated with LSEC capillarization, which promotes basement membrane formation while decreasing permeability.[21,22] There was significant upregulation of LSEC markers associated with capillarization, including CD31, vascular endothelial growth factor (VEGF), ICAM1 (Intercellular Adhesion Molecule-1), stabilin2, ID1 (Inhibitor of DNA Binding-1), Gata4, and Ehd3 (EH Domain Containing-3) in $F8^{TKO}$ mice by quantitative reverse transcription polymerase chain reaction (qRT-PCR) and western blot (Figure 2E-F; supplemental Figure 1G). qRT-PCR also confirmed the upregulation of basement membrane markers collagen types I (α1), III (α1), and α-smooth muscle actin in the liver of $F8^{TKO}$ mice (supplemental Figure 1D). Finally, immunostaining for the LSEC markers PECAM and LYVE1 demonstrated increased LSCE capillarization in $F8^{TKO}$ mice. As a result of the morphological modification of those cells, staining for both Lyve1 and PECAM (Figure 2G-H) was enhanced throughout the liver tissue, suggestive of increased LSEC capillarization. Our current study is the first to highlight endothelial maladaptive structural changes in FVIII-deficient mice and their deleterious impact on the efficacy of liver-directed gene transfer. Indeed, abnormal endothelial function was recently recognized in patients with hemophilia.[23] Our current findings will inspire future investigations looking at the molecular mechanism underlying loss of endothelial fenestration associated with FVIII deficiency and whether or how this possibly could be affecting liver gene therapy in hemophilia.

Acknowledgments

The authors thank Pete Lollar at Emory University for providing breeding pairs of $F8^{TKO}$ mice, and Mark T. Gladwin for useful suggestions on our preliminary data.

This work was supported by VMI pilot grant P3HVB, National Institutes of Health (NIH), National Institute of Diabetes and Digestive and Kidney Diseases grant K01NIH-NIDDK125617, ASH Junior Faculty Scholar Award (T.P.-S.), NIH, National Heart, Lung, and Blood Institute grants R01HL128297 (P.S.), R01HL141080 (P.S.), R01HL124021 (S.Y.C.), and HL122596 (S.Y.C.); American Heart Association (AHA) grant 18TPA34170588 (P.S.); AHA predoctoral fellowship 19PRE34430188 (R.V.); AHA postdoctoral fellowship AHA828786 (T.W.K.). This work was also supported by the Bayer Hemophilia Award (P.S.); the AHA grant 18EIA33900027 (S.Y.C.); and in part by Health Resources & Services Administration HRSA H30MC2450-04-00 to the Vascular Medicine Institute from the Hemophilia Center of Western Pennsylvania (P.S., T.P.-S.) and by Vitalant (P.S.).

Authorship

Contribution: T.P.-S. conceived and designed the study; T.W.K., R.V., E.-M.J., S.G., S.A., J.F., and T.P.-S. acquired the data; T.P.-S. analyzed and interpreted the data; E.T. and O.K. oversaw breeding the $F8^{TKO}$ mice; J.F. conducted the SEM imaging; T.B. provided reagent; R.K.D. performed experiments; T.P.-S. drafted the manuscript; E.M.N., M.V.R., and P.S. critically reviewed and edited the manuscript; D.B.S., S.C.W., S.Y.C., E.M.N., and P.S. provided technical and material support; E.M.-J. and T.W.K. performed the statistical analysis; and T.P.-S. and P.S. obtained funding.

Conflict-of-interest disclosure: P.S. is a recipient of 2021 Basic Sciences Research Award from Bayer Hemophilia Award Program (BHAP) of Bayer Corp and funding (not relevant to the current study) as a part of sponsored research agreements with CSL Behring Inc, IHP Therapeutics, and Novartis AG. S.Y.C. has served as a consultant for Acceleron Pharma and United Therapeutics; is a director, officer, and shareholder in Synhale Therapeutics; and has held research grants from Actelion, Bayer, and Pfizer. M.V.R. receives research funding from Sanofi, BioMarin, SPARK, and Takeda Pharmaceuticals USA and serves on advisory boards of Sanofi, BioMarin, SPARK, and Takeda Pharmaceuticals USA. The remaining authors declare no competing financial interests.

ORCID profiles: S.C.W., 0000-0003-4092-1552; S.Y.C., 0000-0002-9520-7527; P.S., 0000-0001-7568-5719; T.P.-S., 0000-0002-8763-4844.

Correspondence: Tirthadipa Pradhan-Sundd, Division of Hematology-Oncology, Department of Medicine, Vascular Medicine Institute, University of Pittsburgh School of Medicine, 200 Lothrop Street, Pittsburgh, PA 15261; e-mail: tip9@pitt.edu.

Figure 2 (continued) F8TKO mice show defenestrated vascularized LSEC with decreased permeability. (A) Liver intravital imaging of control and $F8^{TKO}$ liver at baseline and 15 days post–AAV8-GFP administration injected with TXR-dextran and AF488-anti-CD31. (B) SEM images show LSEC fenestrae are significantly less in a representative $F8^{TKO}$ mouse as compared with a control mouse. (C) SEM images show LSEC fenestrae are significantly less in a representative *B6; 129S-F8tm1Kaz/J* mouse as compared with a control mouse. (D) Quantification of pore grouping and total number of fenestrae per field of view in the liver of control *B6; 129S-F8tm1Kaz/J* and $F8^{TKO}$ mice. (E) Heatmap consisting of qRT-PCR analysis of endothelial-specific genes (CD31, VEGF, ICAM1, stabilin2, ID1, Gata4, and Ehd3) in control and $F8^{TKO}$ mice liver. (F) Western blot analysis of VEGF and CD31 in control and $F8^{TKO}$ mice at baseline. Immunofluorescence for PECAM (G) and LYVE-1 (H) showed an increased accumulation in $F8^{TKO}$ mouse liver tissue at baseline, which was not seen in age-matched control liver. All control mice used were unaffected littermate heterozygoes mice.

References

1. Srivastava A, Brewer AK, Mauser-Bunschoten EP, et al; Treatment Guidelines Working Group on Behalf of The World Federation Of Hemophilia. Guidelines for the management of hemophilia. *Haemophilia.* 2013;19(1):e1-e47.
2. Samuelson Bannow B, Recht M, Négrier C, et al. Factor VIII: long-established role in haemophilia A and emerging evidence beyond haemostasis. *Blood Rev.* 2019;35:43-50.
3. Pradhan-Sundd T, Gudapati S, Kaminski TW, Ragni MV. Exploring the complex role of coagulation factor VIII in chronic liver disease. *Cell Mol Gastroenterol Hepatol.* 2021;12(3):1061-1072.
4. Nathwani AC. Gene therapy for hemophilia. *Hematology Am Soc Hematol Educ Program*. 2019;2019:1-8.
5. Manno CS, Pierce GF, Arruda VR, et al. Successful transduction of liver in hemophilia by AAV-Factor IX and limitations imposed by the host immune response [published correction appears in *Nat Med*. 2006;12(5):592]. *Nat Med.* 2006;12(3):342-347.
6. Ohmori T. Advances in gene therapy for hemophilia: basis, current status, and future perspectives. *Int J Hematol.* 2020;111(1):31-41.
7. Perrin GQ, Herzog RW, Markusic DM. Update on clinical gene therapy for hemophilia. *Blood.* 2019;133(5):407-414.
8. Ragni MV. Hemophilia as a blueprint for gene therapy. *Science.* 2021;374(6563):40-41.
9. Rangarajan S, Walsh L, Lester W, et al. AAV5-factor VIII gene transfer in severe hemophilia A. *N Engl J Med.* 2017;377(26):2519-2530.
10. Varthaman A, Lacroix-Desmazes S. Pathogenic immune response to therapeutic factor VIII: exacerbated response or failed induction of tolerance? *Haematologica.* 2019;104(2):236-244.
11. Chen J, Peterson RT, Schreiber SL. Alpha 4 associates with protein phosphatases 2A, 4, and 6. *Biochem Biophys Res Commun.* 1998;247(3):827-832.
12. Jiang H, Lillicrap D, Patarroyo-White S, et al. Multiyear therapeutic benefit of AAV serotypes 2, 6, and 8 delivering factor VIII to hemophilia A mice and dogs. *Blood.* 2006;108(1):107-115.
13. Mazurkiewicz-Pisarek A, Płucienniczak G, Ciach T, Płucienniczak A. The factor VIII protein and its function. *Acta Biochim Pol.* 2016;63(1):11-16.
14. Chao BN, Baldwin WH, Healey JF, et al. Characterization of a genetically engineered mouse model of hemophilia A with complete deletion of the F8 gene. *J Thromb Haemost.* 2016;14(2):346-355.
15. Pradhan-Sundd T, Vats R, Russell JO, et al. Dysregulated bile transporters and impaired tight junctions during chronic liver injury in mice. *Gastroenterology.* 2018;155(4):1218-1232.e24.
16. Pradhan-Sundd T, Zhou L, Vats R, et al. Dual catenin loss in murine liver causes tight junctional deregulation and progressive intrahepatic cholestasis. *Hepatology.* 2018;67(6):2320-2337.
17. Duan D. Systemic delivery of adeno-associated viral vectors. *Curr Opin Virol.* 2016;21:16-25.
18. Zapotoczny B, Szafranska K, Kus E, et al. Tracking fenestrae dynamics in live murine liver sinusoidal endothelial cells. *Hepatology.* 2019;69(2):876-888.
19. Poisson J, Lemoinne S, Boulanger C, et al. Liver sinusoidal endothelial cells: physiology and role in liver diseases. *J Hepatol.* 2017;66(1):212-227.
20. Kren BT, Unger GM, Sjeklocha L, et al. Nanocapsule-delivered Sleeping Beauty mediates therapeutic Factor VIII expression in liver sinusoidal endothelial cells of hemophilia A mice. *J Clin Invest.* 2009;119(7):2086-2099.
21. Braet F, Wisse E. Structural and functional aspects of liver sinusoidal endothelial cell fenestrae: a review. *Comp Hepatol.* 2002;1(1):1.
22. Xu B, Broome U, Uzunel M, et al. Capillarization of hepatic sinusoid by liver endothelial cell-reactive autoantibodies in patients with cirrhosis and chronic hepatitis. *Am J Pathol.* 2003;163(4):1275-1289.
23. Böhmert S, Schubert R, Fichtlscherer S, Alesci S, Miesbach W. Endothelial function in patients with severe and moderate haemophilia A and B. *Hamostaseologie.* 2019;39(2):195-202.